Optics and Laser Technology 131 (2020) 106462

Contents lists available at ScienceDirect

Optics and Laser Technology

journal homepage: www.elsevier.com/locate/optlastec

Full length article

Optical characteristics and dispersion parameters of thermally evaporated $Ge_{50}In_4Ga_{13}Se_{33}$ chalcogenide thin films

E.G. El-Metwally*, E.M. Assim, S.S. Fouad

Department of Physics, Faculty of Education, Ain Shams University, Cairo 11566, Egypt

HIGHLIGHTS

- Both refractive index n and extinction coefficient k are thickness independent.
- The indirect optical energy gap value E_g^{opt} is 1.527 eV for $Ge_{50}In_4Ga_{13}Se_{33}$ films.
- Dispersion energy parameters and the lattice dielectric constant ε_L were obtained.
- Values of the 3rd order optical susceptibility $\chi^{(3)}$ and n_2 were calculated.
- Variation of ε_1, ε_2, $tan\delta$, τ, σ_{opt}, V_{ELF} and S_{ELF} with photon energy were studied.

ARTICLE INFO

Keywords:
Chalcogenide glasses
Amorphous semiconductors
Optical constants
Linear and non-linear optics

ABSTRACT

$Ge_{50}In_4Ga_{13}Se_{33}$ glassy composition was fabricated using the chemical composition and the melt quenching technique. Using X-ray diffraction (XRD) and energy dispersive X-ray (EDX) analysis, the structural characterization of the thermally evaporated films with different thicknesses (126–745 nm) used in this study was determined. Transmittance $T(\lambda)$ spectrum was obtained in the range of wavelength from 400 nm to 2500 nm at room temperature. Swanepoel's method was employed to evaluate the optical constants, refractive index n and extinction coefficient k. From the obtained data of n, transmission coefficient T_C and reflection loss factor R_L were determined. Optical band gap E_g^{opt} and Urbach tail E_u were determined using Tauc's extrapolation method. The calculated value of the transition power factor p revealed the indirect optical transition indicated in this study. The Wemple-DiDomenico parameters are also reported for the composition under study. The dependency of real ε_1 and imaginary ε_2 components of dielectric constant, dissipation factor $tan\delta$, relaxation time τ volume and surface energy loss functions and the optical conductivity σ_{opt} on photon energy $h\nu$ were studied also for $Ge_{50}In_4Ga_{13}Se_{33}$ films. In addition, the 3rd order non-linear optical susceptibility $\chi^{(3)}$ and non-linear refractive index n_2 were determined.

1. Introduction

The exceptional optical properties of chalcogenide glasses like high non-linear refractive, widely optical transmission window and low energy of phonons were the essential reason to use it for photonics applications [1]. Chalcogenide glasses are generally utilized in a many optoelectronic applications, for example, in the assembling of inexpensive solar cells, photonic circuits, infrared optical fibers, signal preparing, as reversible phase change optical recorders, micro sensing, photolithography, switching and memory devices, electro-chemical sensors, biomedical applications, photovoltaics, LED, waveguides, holography and IR detectors [2–8]. Because of the applications of chalcogenide glasses in the development of information technology, optical characterization attracts much attention in research [9–14]. The composition $Ge_{50}In_4Ga_{13}Se_{33}$ is new generation in semiconductor chalcogenide devices which can provide many physical properties as there is a lack of information about it. It is known that chalcogenide-based glasses have attained great interest because of its electrical, optical, thermal, and optoelectronic properties, these semiconducting glasses have many industrial applications [5]. Therefore, we try to explore some physical properties of this compound for industrial use applications as a new addition and the switching phenomenon measurements that are expected to be promising in the future.

Tintu et al. [15], studied the photo-induced properties on the $Ga_5Sb_{10}Ge_{25}Se_{60}$ thin films and suggested that the optical band gap E_g^{opt} depends on the power and duration of laser radiation, as well as the

* Corresponding author.
E-mail address: eg_elmetwally@yahoo.com (E.G. El-Metwally).

https://doi.org/10.1016/j.optlastec.2020.106462
Received 26 February 2020; Received in revised form 9 June 2020; Accepted 25 June 2020

increase in the index of refraction n, which may be due to the photo-darkening process in the studied composition. Bin Ye et al. [16], reported the effect of Se content on optical and thermo-mechanical properties of Ge-Ga-Sb-S chalcogenide glass and found that thermal stability against crystallization and widening in the infrared transmission region can be significantly enhanced by the replacing Se with S in Ge-Ga-Sb glasses. Shiryaev et al. [17], studied the micro-structure, the edges of the transmission spectrum, the optical band gap energy E_g^{opt} and the index of refraction n for $Ga_xGe_{25}As_{15}Se_{60-x}$ (x = 0–5) glasses and concluded that the refractive index n increased as Se was replaced by Ga. Tverjanovich et al. [18], had been studied photo-induced bleaching in Ga-Ge-S (Se) films and reported that, exposure of the examined films to radiation energy greater than their band gap leads to bleaching of S-based films due to the local film oxidation, while replacing S by Se in the composition of films results in the opposite effect: irradiation of films results in photo-induced darkening. Ekta Sharma et al. [19], studied $Ge_{10}Te_{80}Se_{10-x}Ga$ (x = 0, 2, 4, 6, 8, 10 at%) system and reported a decrease in the energy band gap with an increase in Ga (at.%) and behaviour associated with a decrease in both the average single bond energy from 72.71 J/mol to 69.7 J/mol as well as the electronegativity from 2.14 to 2.06 for the investigated system. In all glassy materials, the 3rd order susceptibility $\chi^{(3)}$ as a predominant non-linearity is generated by excitation in the transparent region of frequency, much below the band gap E_g^{opt} and can also be calculated approximately from linear index of refraction n or linear optical susceptibility $\chi^{(1)}$ [20].

In this paper, we present a study on the structure and optical characterization of $Ge_{50}In_4Ga_{13}Se_{33}$ films. In this regard, $Ge_{50}In_4Ga_{13}Se_{33}$ films were not previously studied the best of our knowledge. The relationship between the refractive index n and other associated parameters such as the transmission coefficient T_C and the reflection factor R_L was investigated. The type of optical transitions and the optical band gap E_g^{opt} value have been identified for $Ge_{50}In_4Ga_{13}Se_{33}$ films. Values of the index of refraction n were analyzed in the normal dispersion region to determine the optical energy dispersion parameters (E_o and E_d), averages of inter-band oscillator wavelength λ_0 and oscillator strength S_o, the optical high-frequency and the lattice dielectric constant (ε_∞ and ε_L). The dependency of the dielectric constant ε_1, dielectric loss ε_2, dissipation factor $tan\delta$, time of relaxation τ, volume energy loss function (V_{ELF}), surface energy loss function (S_{ELF}) and the optical conductivity σ_{opt} on photon energy $h\nu$ was studied in the fundamental region and near the fundamental edge. The relation between the linear n and non-linear refractive index n_2 was discussed and the values of the 3rd order non-linear optical susceptibility $\chi^{(3)}$ and n_2 were calculated for thin $Ge_{50}In_4Ga_{13}Se_{33}$ films.

2. Experimental procedures

The melt-quenching technique was used to prepare $Ge_{50}In_4Ga_{13}Se_{33}$ bulk glass from Ge, In, Ga and Se elements of high purity (99.999%) from Aldrich (Co, UK). Based on their atomic percentage, the previous elements were weighed and then sealed into evacuated (10^{-3} Pa) silica tube. The tube was gradually heated up to 1273 K for 20 hrs in an oscillatory furnace. Then the tube was quenched in iced water to produce an amorphous specimen. Coating unit (Edward E306A) was used to obtain the thin films of the bulk sample on glass substrates by thermal evaporation method under vacuum. Tolansky's method [21] used to estimate the film thickness of the samples under study. The amorphous nature of the investigated film samples was assured by using X-ray diffractometer (PANalytical Philips X'Pert PRODIFFRACTOMETER). The chemical composition of the studied composition was investigated by the energy dispersive X-ray (EDX) spectroscopy using (JOEL 5400 - SEM). Using a double beam spectrophotometer (JASCO V-670) in the range of wavelength of 400 nm to 2500 nm, unpolarized light at normal incidence was used to measure the spectral distribution of transmittance $T(\lambda)$ at room temperature (303 K) for $Ge_{50}In_4Ga_{13}Se_{33}$ films of various thicknesses from 126 nm to 745 nm. The experimental error in the measure of film thickness as well as transmittance $T(\lambda)$ is ± 2%.

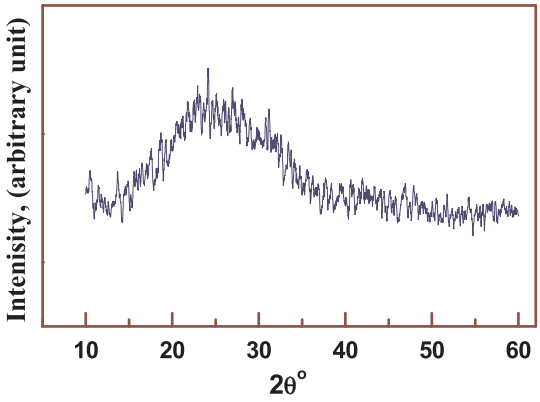

Fig. 1. X-ray diffraction (XRD) pattern of $Ge_{50}In_4Ga_{13}Se_{33}$ thin film sample.

3. Results and discussion

3.1. Structural characterization of $Ge_{50}In_4Ga_{13}Se_{33}$ films

The XRD pattern of thin $Ge_{50}In_4Ga_{13}Se_{33}$ film is shown in Fig. 1. The amorphicity of the investigated film samples has been confirmed due to the absence of any sharp peaks. Using the EDX analysis, the homogeneity of bulk and thin film samples was checked by determining the elementary composition under study in arbitrary areas on the surface of the sample. Table 1 indicates the percentages of the constituent elements considered to be proximate to the prepared composition.

3.2. Optical absorption coefficient, energy band gap and Urbach energy for $Ge_{50}In_4Ga_{13}Se_{33}$ films

The spectral distribution of transmittance $T(\lambda)$ for thin $Ge_{50}In_4Ga_{13}Se_{33}$ films of various thicknesses in the range (126–745 nm) is shown in Fig. 2. In this work, the method suggested by Swanepoel's [22] was used to estimate the refractive index n values as well as the extinction coefficient k. The evaluated values of n and k are not depending on the thickness of film in the studied range, since the variation in the parameter values do not exceed the experimental errors ± 1.0%, as seen in Figs. 3 and 4. It is obvious from Fig. 3 that, n decreases with increasing the wavelength suggesting the usual dispersion behaviour of n is considered an indication of the existence of multiple interactions in the investigated composition between the electrons and incident photons.

The coefficient of transmission T_C represents the overall transmitted wave power compared to an incident wave or defines the intensity of the amplitude. According to Linda et al. [23] one can get an equation describes the relation between the refractive index n and the transmission coefficient T_C, as follows:

$$T_C = 2n/(n^2 + 1) \quad (1)$$

The reflection (return) loss factor R_L, is the ratio of reflected power to incident power, in other word it is the loss power in the signal returned by a discontinuity in a transmission line. The reflection factor R_L is also related to the refractive index n according to the following

Table 1
The EDX data of $Ge_{50}In_4Ga_{13}Se_{33}$ films.

Element	Ge	In	Ga	Se
Atomic %	49.47	4.20	13.02	33.31

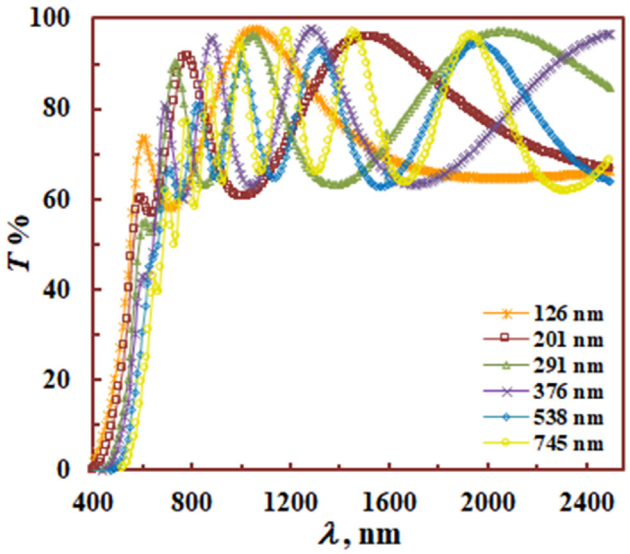

Fig. 2. Spectral distribution of transmission $T(\lambda)$ for $Ge_{50}In_4Ga_{13}Se_{33}$ films of different thicknesses.

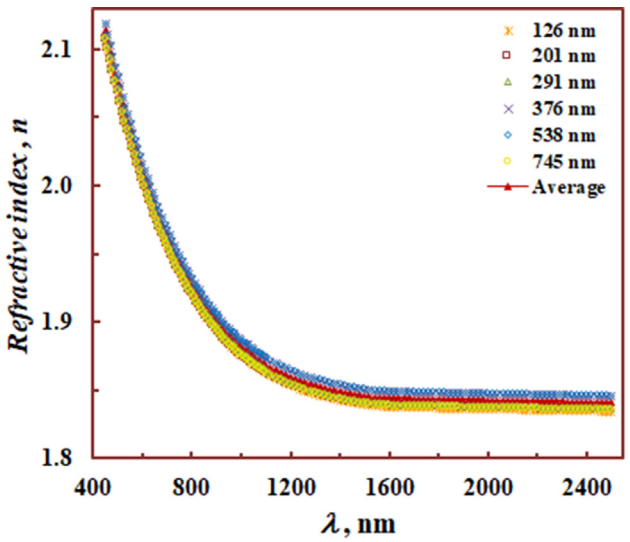

Fig. 3. The dependence of the refractive index n on λ for $Ge_{50}In_4Ga_{13}Se_{33}$ films of different thicknesses and its average values.

empirical equation [24]:

$$R_L = [(n-1)/(n+2)]^2 \quad (2)$$

Considering equations (1&2) the relationship between the transmission coefficient T_C and the reflection loss factor R_L presented in Fig. 5. This relation shows an inverse proportionality between the two quantities as expected. Study of the optical absorption coefficient α gives important details on the energy gap and the band structure of the material, which is related to the extinction coefficient k by the well-known equation $\alpha = 4\pi k/\lambda$. The graphical presentation of α versus photon energy $h\nu$ for $Ge_{50}In_4Ga_{13}Se_{33}$ films is illustrated in Fig. 6. For values of $\alpha \geq 10^4 cm^{-1}$, the absorption is attributed to transitions between extended states in both conduction and valence bands. The optical energy gap E_g^{opt} could be evaluated using equation [25,26]:

$$(\alpha h\nu)^{1/p} = B(h\nu - E_g^{opt}) \quad (3)$$

where B is a constant and p is the power factor of the transition mode, that depends mainly upon the structure of the prepared sample [27]. The power p has the value of (1/2) and (2) for direct and indirect

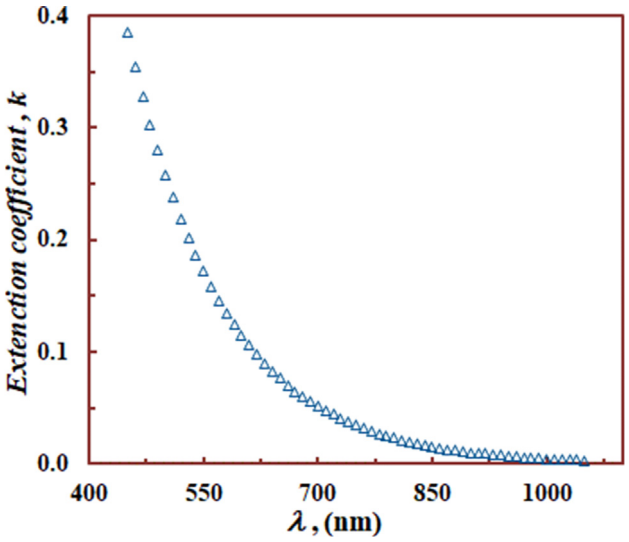

Fig. 4. The dependence of the average values of the extinction coefficient k on λ for $Ge_{50}In_4Ga_{13}Se_{33}$ films.

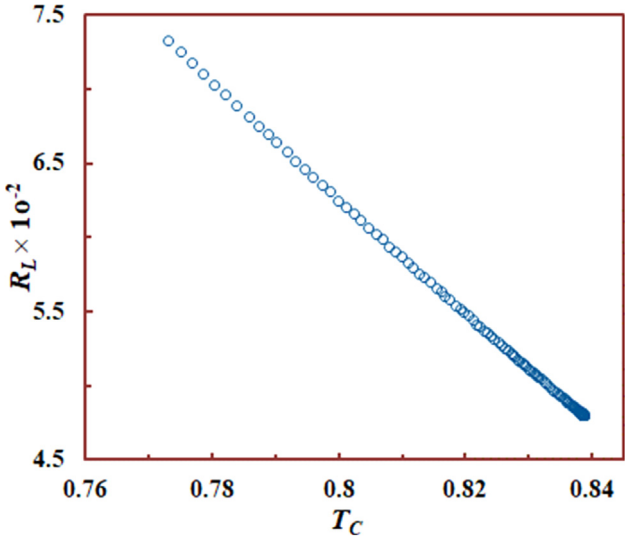

Fig. 5. The reflection loss factor R_L as a function of transmission coefficient T_C for $Ge_{50}In_4Ga_{13}Se_{33}$ films.

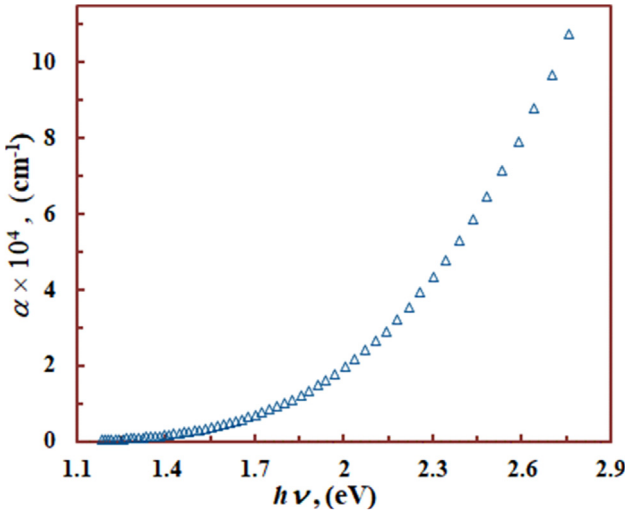

Fig. 6. Plots of α as a function of photon energy $h\nu$ for $Ge_{50}In_4Ga_{13}Se_{33}$ films.

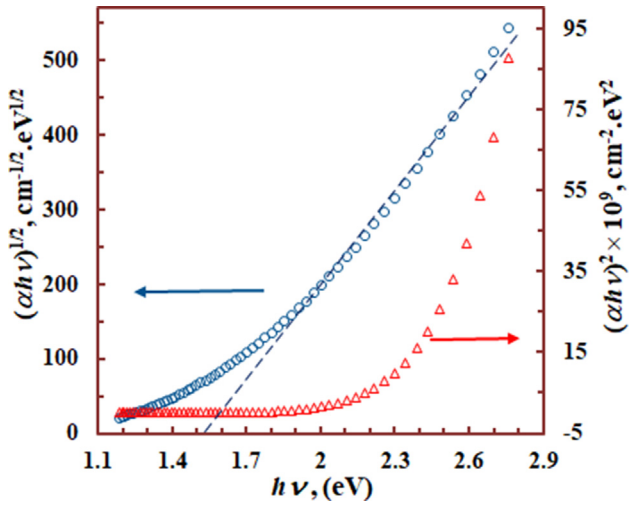

Fig. 7. Dependence of $(\alpha h\nu)^{1/2}$ on the photon energy $h\nu$ for $Ge_{50}In_4Ga_{13}Se_{33}$ films.

Table 2
Values of the optical energy gap E_g^{opt}, the constant B, the Urbach energy E_u and the constant α_o for thin $Ge_{50}In_4Ga_{13}Se_{33}$ films.

Parameter	E_g^{opt}, eV	B,cm^{-1} eV^{-1}	E_u,eV	α_o, cm^{-1}
Value	1.527 ± 0.020	1.79 × 10^5	0.182 ± 0.010	0.656

transitions, respectively. To evaluate the value of E_g^{opt}, relationships $(\alpha h\nu)^{1/2}$ and $(\alpha h\nu)^2$ versus $h\nu$ are plotted in Fig. 7 for thin $Ge_{50}In_4Ga_{13}Se_{33}$ films. It can be seen that, the relation $(\alpha h\nu)^{1/2} = f(h\nu)$ is linear, which denotes that the allowed transitions in the studied films are indirect. Values of the optical band gap E_g^{opt} and the constant B were obtained by extrapolating the linear part of the relationship between $(\alpha h\nu)^{1/2}$ and $h\nu$ at $(\alpha h\nu)^{1/2} = 0$ and from the slope of the linear portion of this relation, respectively. The calculated values of E_g^{opt} and B are listed in Table 2.

In order to verify the power factor or the transition factor p we can use the following empirical equation [27]:

$$\ln(\alpha h\nu) = lnC + p\ ln(h\nu - E_g^{opt}) \quad (4)$$

Fig. 8 shows that the empirical relation of the linear relationship is

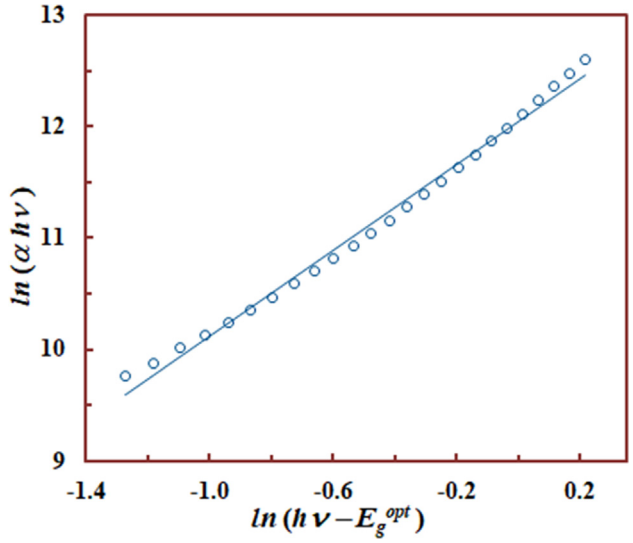

Fig. 8. Plot of $ln(\alpha h\nu)$ as a function of $ln(h\nu - E_g^{opt})$ for $Ge_{50}In_4Ga_{13}Se_{33}$ films.

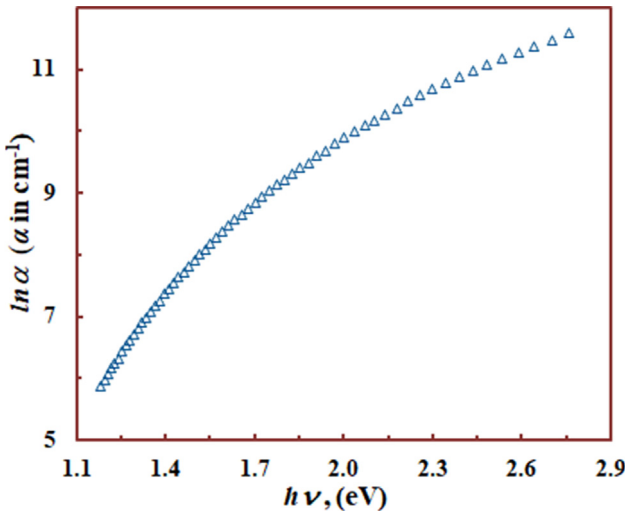

Fig. 9. Plots of $ln\alpha$ as a function of photon energy $h\nu$ for $Ge_{50}In_4Ga_{13}Se_{33}$ films.

valid and the calculated value of the transition power factor p estimated from the slope of the straight line of Fig. 8 is ≈1.96, or approximately equal 2. The calculated value of the power p confirms that, the allowed transitions are indirect for $Ge_{50}In_4Ga_{13}Se_{33}$ films as mentioned above from Fig. 7 and Eq. (3).

For values of $\alpha < 10^4$ cm^{-1}, the absorption is attributed to the transition between localized states and depends mainly on the photon energy according to Urbach relation [28]:

$$\alpha(\nu) = \alpha_0 \exp(h\nu/E_u) \quad (5)$$

where α_0 is a constant and E_u is the Urbach energy tail representing the degree of disordered in non-crystalline materials [28]. Values of E_u and α_o are calculated from the slope of the linear part and the intercept with y-axis of the graphical presented between $ln\alpha$ and $h\nu$, respectively as illustrate in Fig. 9, and given in Table 2.

3.3. Optical dispersion parameters of $Ge_{50}In_4Ga_{13}Se_{33}$ films

The spectral distribution of n in the normal dispersion region at lower optical frequencies was analyzed using the single effective oscillator model established by Wemple and DiDomenico (WDD) [29,30]. This model assumes that the index of refraction n of the studied films is linked to the single-oscillator E_o and dispersion E_d energies by the following equation [30–32]:

$$(n^2 - 1)^{-1} = \frac{[E_o^2 - (h\nu)^2]}{E_o E_d} \quad (6)$$

The graphical presentation of $(n^2 - 1)^{-1}$ versus $(h\nu)^2$ for the films under study is shown in Fig. 10. As seen, the obtained slope of the straight line is $(E_0E_d)^{-1}$ and the intercept with y-axis is (E_0/E_d). The deduced values of E_o and E_d are given in Table 3. The acquired bend demonstrates a divergence from linearity at longer wavelengths might be because of the negative contributions of the vibrations of lattice to the index of refraction [29,30]. According to WDD model, values of both the static refractive index n_o (at $h\nu \to 0$) and the high-frequency dielectric constant ε_∞ for the films under investigation are determined from equations: $n_o = \sqrt{1 + (E_d/E_o)}$ and $\varepsilon_\infty = n_o^2$, respectively and given in Table 3. Also, the oscillator strength $\mathscr{F}$ is an important parameter reported by Wemple and DiDomenico [33] as: $\mathscr{F} = E_oE_d$ is calculated for $Ge_{50}In_4Ga_{13}Se_{33}$ films and listed in Table 3.

The refractive index n can also be investigated to estimate the averages of inter-band oscillator wavelength λ_0 and oscillator strength S_o in the transparent region for the studied films. The index of refraction n is correlated with the wavelength λ according to Sellmeier's dispersion relation as following [34–36]:

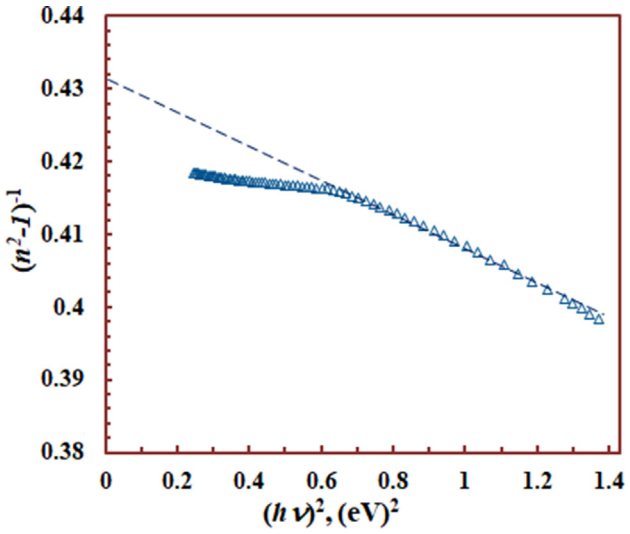

Fig. 10. A plot of $(n^2-1)^{-1}$ against $(h\nu)^2$ for $Ge_{50}In_4Ga_{13}Se_{33}$ films.

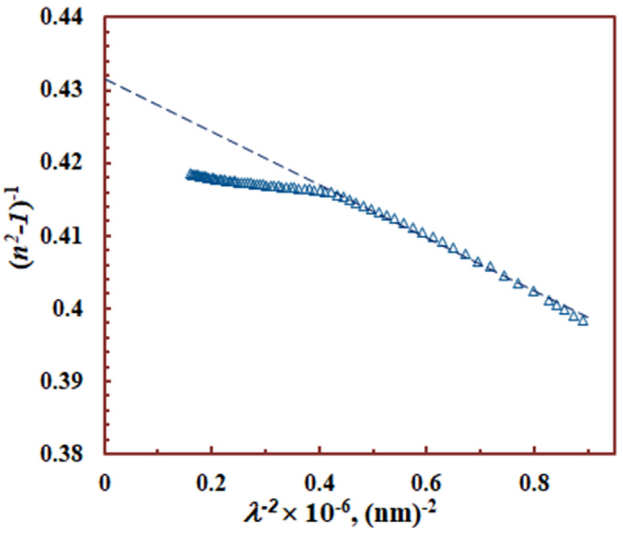

Fig. 11. A plot of $(n^2-1)^{-1}$ as a function of λ^{-2} for $Ge_{50}In_4Ga_{13}Se_{33}$ films.

$$(n^2-1)^{-1}=\frac{[1-(\lambda_o/\lambda)^2]}{(n_o^2-1)} \tag{7}$$

where,

$$(n_o^2-1)=S_o\lambda_o^2 \tag{8}$$

From the relation between $(n^2-1)^{-1}$ and λ^{-2} for $Ge_{50}In_4Ga_{13}Se_{33}$ films as shown in Fig. 11 we can determine the values of λ_0 and S_o from the slope of the linear part of the curve of this figure and Eq. (8), respectively. The estimated values of λ_0 and S_o are presented in Table 3.

In the non-absorbing (transparent) region ($k=0$), the dielectric constant is attributed to both free electrons and bound electrons. The relationship n^2 and λ^2 is defined by [34]:

$$n^2=\varepsilon_L-\left(\frac{e^2}{4\pi^2\varepsilon_0 c^2}\right)\left(\frac{N}{m^*}\right)\lambda^2 \tag{9}$$

where ε_L is the lattice dielectric constant, e is the electronic charge, N/m^* is the ratio of free charge-carriers concentration and its effective mass and c is the speed of light. We can calculate the values of ε_L and (N/m^*) by plotting the relation between n^2 and λ^2 from the intersection and the slope of linear portion of this curve, respectively as appeared in Fig. 12. The obtained values of ε_L and (N/m^*) for $Ge_{50}In_4Ga_{13}Se_{33}$ films are given in Table 4. It is found that the value of ε_L is greater than the value of ε_∞ which attributed to the participation of free charged carriers in the process of polarization that takes place within the material when the light is incidental to it [37,38].

The plasma frequency ω_p is known as the frequency of the resonance of the electron free oscillations of around their positions of equilibrium and is defined by [8,39]:

$$\omega_p=\left(\frac{e^2N}{\varepsilon_0\varepsilon_\infty m^*}\right)^{\frac{1}{2}} \tag{10}$$

Utilizing the N/m^* value provided in Table 4, Eq. (10) is used to determine ω_p and is included in the same table as well.

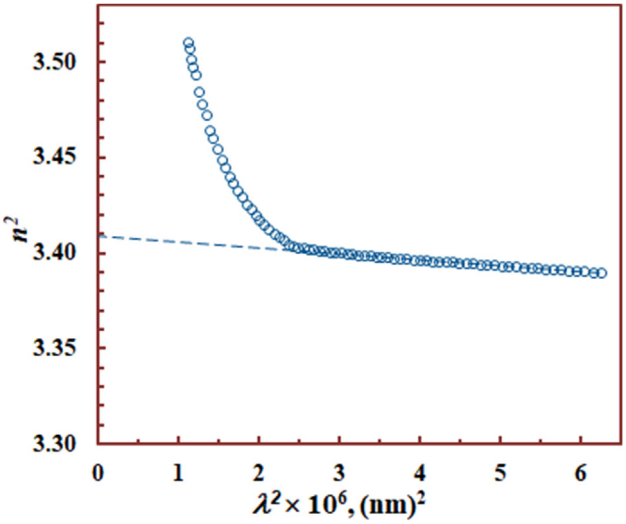

Fig. 12. A plot of n^2 as a function of λ^2 for $Ge_{50}In_4Ga_{13}Se_{33}$ films.

3.4. Non-linear optical (NLO) properties of $Ge_{50}In_4Ga_{13}Se_{33}$ films

The non-linear phenomenon happens when the medium is propagated by the high light intensity. The non-linearity is expressed in the material's polarization. Consequently, the polarization is no longer linear proportional to the incident photon electrical field E. For example, optical power limiting, optical switching, image processing and image manipulation are various applications on this phenomenon [38,40].

The 3rd order non-linear optical susceptibility $\chi^{(3)}$ can be calculated from the parameters of dispersion energy (E_o and E_d) and was experimentally investigated on a wide variety of materials such as semiconductors, glasses-doped semiconductor, homogeneous bulk glasses, polymers and nanomaterials [41], which is an extremely important basis for a variety of technologies, including high-capacity

Table 3
Values of the oscillator energy E_o, the dispersion energy E_d, the oscillatory strength $\mathscr{F}$, the static refractive index n_o, the infinite dielectric constant ε_∞, the interband oscillator wavelength λ_0 and the average oscillator strength S_o for thin $Ge_{50}In_4Ga_{13}Se_{33}$ films.

Parameter	E_o, eV	E_d, eV	$\mathscr{F}$, eV^2	n_o	ε_∞	λ_0, nm	S_o, m^{-2}
Value	4.28 ± 0.03	9.93 ± 0.03	42.50	1.822	3.32 ± 0.02	290.2 ± 0.5	2.76×10^{13}

Table 4
Values of the lattice dielectric constant ε_L, the ratio N/m^*, the plasma frequency ω_p, the third order nonlinear optical susceptibility $\chi^{(3)}$ and the non-linear refractive index n_2 for thin $Ge_{50}In_4Ga_{13}Se_{33}$ films.

Parameter	ε_L	N/m^*, $cm^{-3}.g^{-1}$	ω_p, s^{-1}	$\chi^{(3)}$, esu	n_2, esu
Value	3.41 ± 0.02	3.93×10^{45}	5.85×10^{13}	1.98×10^{-13}	4.10×10^{-12}

communications networks [31,42,43]. The value of $\chi^{(3)}$ can be estimated from the following relation according to Miller's generalized rule [44]:

$$\chi^{(3)} = \frac{A}{(4\pi)^4}(n_0^2 - 1)^4 = \frac{A}{(4\pi)^4}\left(\frac{E_d}{E_o}\right)^4 \quad (11)$$

where A is a constant equal to 1.7×10^{-10} esu [44,45], which is supposed to be independent of the frequency and almost the same for other materials. The index of refraction n is equal to n_o in the case of $\chi^{(3)}$ value within the limit of $h\upsilon \to 0$. Tichy et al. [45] combined the Miller's rule and the static index of refraction n_o which was determined by Wemple-DiDominico. The non-linear refractive index n_2 is calculated by [44,45]:

$$n_2 = \frac{12\pi\chi^{(3)}}{n_0} \quad (12)$$

The calculated values of $\chi^{(3)}$ and n_2 at $(h\upsilon \to 0)$ for $Ge_{50}In_4Ga_{13}Se_{33}$ films are presented in Table 4. The non-linear index of refraction n_2 varies from that of linear since n_2 depends on the intensity of the incident light, where the polarization is proportional to the square of the incident light electrical field E^2 rather than is proportional to the electrical field E for linear behaviour.

The calculated value of n_2 for $Ge_{50}In_4Ga_{13}Se_{33}$ films which given in Table 4 in the same order of other as amorphous compositions chalcogenide glasses [46–48], deducing that the investigated composition is an interesting material for applications of the non-linear optics. The obtained results are in good agreement with other amorphous semiconductors for non-linear optical parameters [46–48].

3.5. The complex dielectric constant and optical conductivity near the absorption edge for $Ge_{50}In_4Ga_{13}Se_{33}$ films

The real ε_1 and imaginary ε_2 components of the complex dielectric constants ε^* $(\varepsilon^* = \varepsilon_1 + i\varepsilon_2)$, are associated to the optical dispersion parameters n and k as [34,49]:

$$\varepsilon_1 = n^2 - k^2 \;\&\; \varepsilon_2 = 2nk \quad (13)$$

Fig. 13 represents the dependence of ε_1 and ε_2 on $h\upsilon$ for thin $Ge_{50}In_4Ga_{13}Se_{33}$ films. It is clear that, there is a positive proportional between both ε_1 and ε_2 with $h\upsilon$ and the values of ε_1 are greater than those of ε_2. The variation of the dielectric constant with the energy of photons $h\upsilon$ can be attributed to the interactions that are generated in the film between electrons and the incident photons.

The dissipation factor or the loss tangent $tan\delta$ is a measure of a mechanical mode's power loss rate, like oscillations in a dissipate device, and can be determined by [8,50]:

$$tan\delta = \frac{\varepsilon_2}{\varepsilon_1} \quad (14)$$

Fig. 14 indicates the positive proportional between $tan\delta$ with $h\upsilon$ for the investigated composition, where $tan\delta$ increases with the increase of $h\upsilon$.

The property strongly associated with a solid's conductivity is the dielectric relaxation time τ, which can be determined by [51,52]:

$$\tau = \frac{\varepsilon_\infty - \varepsilon_1}{\omega\varepsilon_2} \quad (15)$$

where ω is the angular frequency. Fig. 15 illustrates the variation of τ with $h\upsilon$ for $Ge_{50}In_4Ga_{13}Se_{33}$ films. It is obvious from this figure that, τ is increment with rising $h\upsilon$.

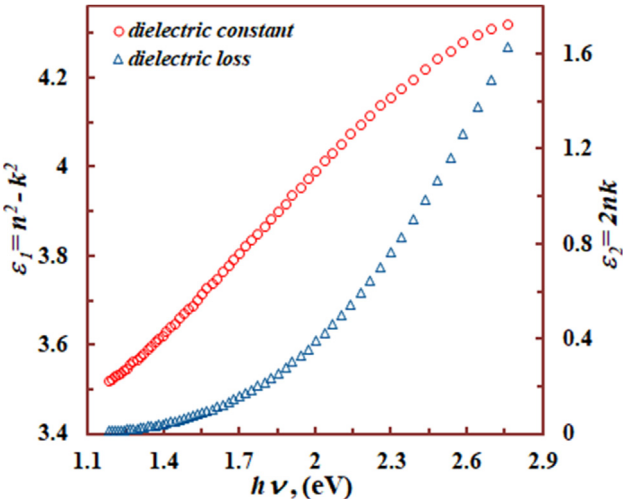

Fig. 13. Plots of ε_1 and ε_2 as a function of the photon energy $h\upsilon$ for $Ge_{50}In_4Ga_{13}Se_{33}$ films.

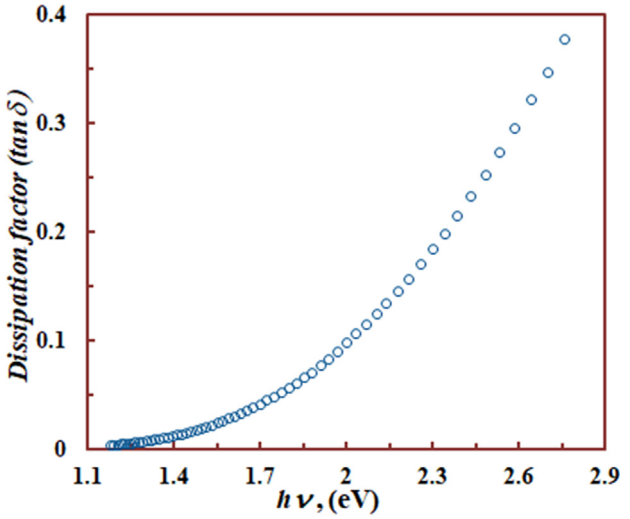

Fig. 14. Dependence of the dissipation factor $tan\delta$ on the photon energy $h\upsilon$ for $Ge_{50}In_4Ga_{13}Se_{33}$ films.

In addition, two quantities, volume (V_{ELF}) and surface (S_{ELF}) energy loss functions define the energy-loss rate of electrons through the material. These quantities are related to ε_1 and ε_2 by the relations [53,54]:

$$V_{ELF} = \frac{\varepsilon_2}{(\varepsilon_1^2 + \varepsilon_2^2)} \quad (16)$$

$$V_{SLF} = \frac{\varepsilon_2}{[(\varepsilon_1^2 + 1)^2 + \varepsilon_2^2]} \quad (17)$$

The dependence of V_{ELF} and S_{ELF} on photon energy $h\upsilon$ for $Ge_{50}In_4Ga_{13}Se_{33}$ films represented in Fig. 16. From this figure it is clear that, both V_{ELF} and S_{ELF} increase with increasing $h\upsilon$ and the loss of energy by free charged carriers when crossing the bulk material is about

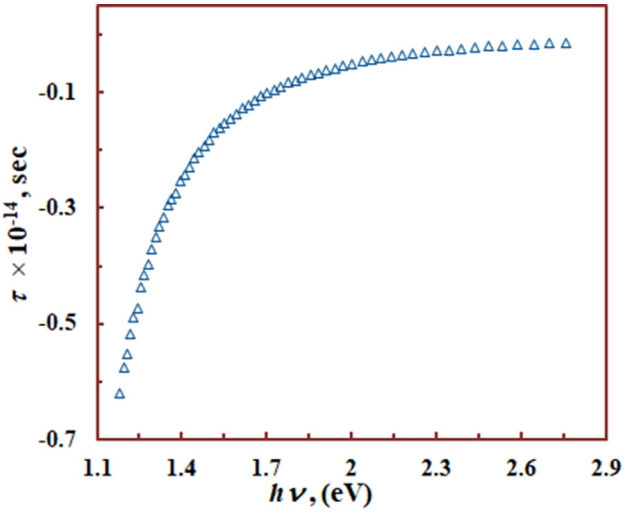

Fig. 15. Dependence of the dielectric relaxation time τ on the photon energy $h\nu$ for $Ge_{50}In_4Ga_{13}Se_{33}$ films.

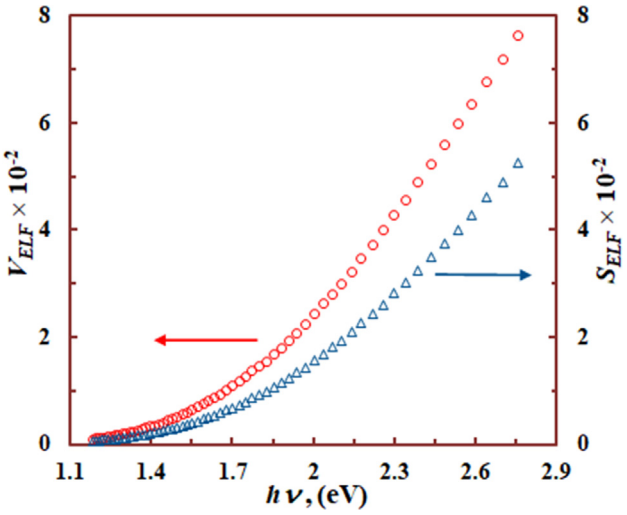

Fig. 16. Variation of V_{ELF} and S_{ELF} as a function of the photon energy $h\nu$ for $Ge_{50}In_4Ga_{13}Se_{33}$ films.

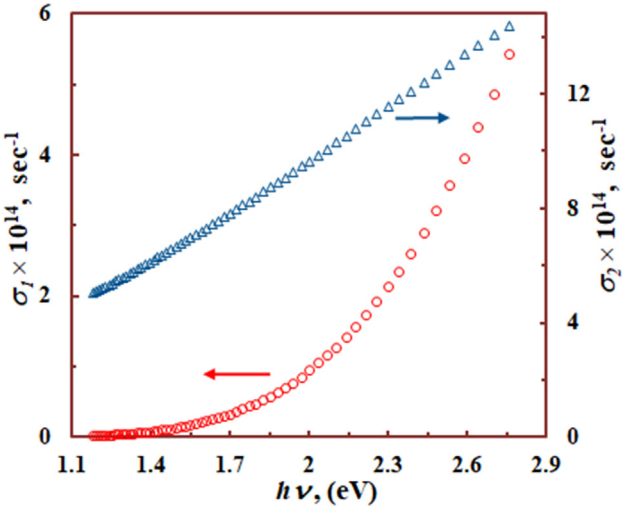

Fig. 17. Dependence of σ_1 and σ_2 on the photon energy $h\nu$ for $Ge_{50}In_4Ga_{13}Se_{33}$ films.

the same as when crossing the surface, especially for lower energy [12,38]. Also, in lower and higher photon energies, there seems to be marked difference between V_{ELF} and S_{ELF}, while V_{ELF} increases more than S_{ELF}.

One of the effective tools used to study the electronic state of a material is optical conductivity. In general, when an external electrical field is exposed to a system, charges and induced currents are redistributed. The induced polarization and currents are proportional to the field induced [55,56]. The real σ_1 and imaginary σ_2 components of complex optical conductivity ($\sigma^* = \sigma_1 + i\sigma_2$) specified by [56–58]:

$$\sigma_1 = \omega\ \varepsilon_o\ \varepsilon_2 \tag{18}$$

$$\sigma_2 = \omega\ \varepsilon_o\ \varepsilon_1 \tag{19}$$

where ε_o is the free space permittivity, which is equal to $(1/4\pi)$ in CGS units. Dependence of σ_1 and σ_2 on photon energy $h\nu$ is presented in Fig. 17. It is evident that, real σ_1 and imaginary σ_2 components of optical conductivity are increased as photon energy $h\nu$ increased this can be attributed to the excitation of electrons by the energy of the incident photons and the changes in the investigated film structure due to the effect of the ordering of charges [56,59,60].

4. Conclusion

The amorphous films of $Ge_{50}In_4Ga_{13}Se_{33}$ of various thicknesses in the range (126–745 nm) were prepared using thermal evaporation method. XRD analysis indicates the amorphous nature of the films under test. The spectral distribution of $T(\lambda)$ for the investigated films of different thicknesses in the studied range was used to calculate the optical constants n and k using Swanepoel's method. The calculated values of n and k for $Ge_{50}In_4Ga_{13}Se_{33}$ films are independent of film thickness. Value of the optical energy gap E_g^{opt} is equal to 1.527 ± 0.020 eV was determined from the analysis of the absorption coefficient α based on Tauc's model. The results obtained indicated that the allowed transitions in the studied films are indirect. Dispersion energy parameters (E_o and E_d), the high-frequency ε_∞ and the lattice ε_L dielectric constants of $Ge_{50}In_4Ga_{13}Se_{33}$ films were obtained. The variation of the dielectric constant, dissipation factor $tan\delta$, relaxation time τ, volume energy loss function (V_{ELF}), surface energy loss function (S_{ELF}) and optical conductivity σ_{opt} with photon energy $h\nu$ were studied. The relation between the non-linear refractive index n_2 and other related parameters were discussed and the values of the 3rd order nonlinear optical susceptibility $\chi^{(3)}$ and n_2 were evaluated for $Ge_{50}In_4Ga_{13}Se_{33}$ films.

Declaration of Competing Interest

The author declare that there is no conflict of interest.

References

[1] N. Donga, Y. Chena, N. Weia, G. Wanga, R.W.S. Daiaa, Qiuhuaiea and Xiang Shena, Infrared Phys. Technol. 86 (2017) 181.
[2] C. Tsay, Y. Zha, C. Arnold, Opt. Express 18 (2010) 26744.
[3] A.S. Hassanien, I. Sharma, A. Alaa, J. Akl, of Non-Cryst. Solids 531 (2020) 119853.
[4] V. Ta'eed, N. Baker, L. Fu, K. Finsterbusch, M. Lamont, D. Moss, H.H. Nguyen, B. Eggleton, D. Choi, S. Madden and B. Luther-Davies, Optics Express 15 (2007) 9205.
[5] Surabhi Mishraa, Pooja Lohiab, D.K. Dwivedia, Infrared Phys. Technol. 100 (2019) 109.
[6] T.K. Todorov, K.B. Reuter, D.B. Mitzi, Adv. Mater. 22 (2010) E156.
[7] A.V. Kolobov, J. Tominaga, Chalcogenides: Metastability and Phase Change Phenomena. Berlin: Springer, 2010.
[8] A.M. Shakra, E.G. El-Metwally, Eur. Phys. J. B 91 (2018) 245.
[9] N.A. Hegab, A.S. Farid, A.M. Shakra, M.A. Afifi, A.M. Alrebati, J. Electron. Mater. 45 (2016) 3332.
[10] A.K. Kukreti, S. Gupta, M. Saxena, N. Rastogi, Int. J. Innovat. Res. Sci. Eng. Technol. 4 (2015) 18608.
[11] B.A. Mansour, S.A. Gada, H.M. Eissa, J. of Non-Cryst. Solids 412 (2015) 53.
[12] H.E. Atyia, N.A. Hegab, Phys. B 454 (2014) 189.
[13] M. Mohamed, Mater. Res. Bull. 65 (2015) 243.
[14] D. Singh, S. Kumar, R. Thangara, J. Phase Transitions 87 (2014) 19.

[15] R. Tintu, V.P.N. Nampoori, P. Radhakrishnan, Sheenu Thomas, Opt. Commun. 284 (2011) 222.
[16] Bin Ye, Shixun Dai, Rongping Wang, Guangming Tao, Xiang Shen, Infrared Phys. Technol. 77 (2016) 21.
[17] V.S. Shiryaev, E.V. Karaksina, M.F. Churbanov, T.V. Kotereva, I.N. Antonov, Mater. Res. Bull. 107 (2018) 430.
[18] A.S. Tverjanovich, E.N. Borisov, O. Volobueva, S.B. Mamedov, M.D. Mikhailov, Glass Phys. Chem 32 (2006) 677.
[19] Ekta Sharma, H.H. Hegazy, Vineet Sharma and Pankaj Sharma, Physica B 562 (2019) 100.
[20] M. Frumor, B. Frumarova, T. Wagner, Comprehensive semiconductor Science and Technology 4 (2011) 206.
[21] S. Tolansky, Multiple-beam Interference Microscopy of Metals, Academic Press, London, 1970.
[22] R. Swanepoel, J. of Physics E: Scientific Instruments 16 (1983) 1214.
[23] D. Linda, J.R. Ducle're, T. Hayakawa, M. Dutreilh-Colas, T. Cardinal, A. Mirgorodsky, A. Kabadou, P. Thomas, J. Alloys Compd. 561 (2013) 151.
[24] B. Bhatia, S.L. Meena, V. Parihar, M. Poonia, New J. Glass and Ceram. 5 (2015) 44.
[25] J. Tauc, Amorphous and Liquid Semiconductors. London and New York: Plenum Press, 1974.
[26] J. Tauc, R. Grigorovici, A. Vancu, Phys. Status Solidi B 15 (1966) 627.
[27] D. Bhattacharya, S. Chaudhuri, A.K. Pal, Vacuum 43 (1992) 313.
[28] F. Urbach, Phys. Rev. 92 (1953) 1324.
[29] M. DiDomenico, S.H. Wemple, J. Appl. Phys. 40 (1969) 720.
[30] S.H. Wemple, M. DiDomenico, Phys. Rev. B 3 (1971) 1338.
[31] M.S. El-Bana, S.S. Fouad, J. Alloys Compd 695 (2017) 1532.
[32] E.R. Shaaban, I.S. Yahia, E.G. El-Metwally, Acta Physica Polonica 121 (2012) 628.
[33] S.H. Wemple, M. DiDomenico Jr., Phys. Rev. B 1 (1970) 193.
[34] J.N. Zemel, J.D. Jensen, R.B. Schoolar, Phys. Rev. 140 (1965) A330.
[35] A.M. Ismail, M.I. Mohammed, E.G. El-Metwally, Indian J. Phys. 93 (2019) 175.
[36] M.M. Abdel-Aziz, E.G. El-Metwally, M. Fadel, H.H. Labib, M.A. Afifi, Thin Solid Films 386 (2001) 99.
[37] A.M. Shakra, H.E. Atyia, M. Fadel, J. Alloys Compd 763 (2018) 983.
[38] M.M. Shehata, H. Kamal, H.M. Hasheme, M.M. El-Nahass, K. Abdelhady, Opt. Laser Technol. 106 (2018) 136.
[39] M.A. Nashera, M.I. Youssif, N.A. El-Ghamaza, H.M. Zeyada, Optik 178 (2019) 532.
[40] E.G. El-Metwally, D.A. Nasrallah, M. Fadel, Mater. Res. Express 6 (2019) 085312.
[41] M.M. El-Nahass, H.S. Soliman, B.A. Khalifa, I.M. Soliman, Mater. Sci. Semicond. Process. 38 (2015) 177.
[42] A. Zawadzka, A. Karakas, P. Plociennik, J. Szatkowski, Z. Lukasiak, A. Kapceoglu, Y. Ceylan, B. Sahraoui, Dyes Pigm. 112 (2015) 116.
[43] S.S. Fouad, G.A.M. Amin, M.S. El-Bana, J. Non-Cryst. Solids 481 (2018) 314.
[44] R.C. Miller, Appl. Phys. Lett. 5 (1964) 17.
[45] L. Tichý, H. Tichá, P. Nagels, R. Callaerts, R. Mertens, M. Vlček, Mater. Lett. 39 (1999) 122.
[46] A.A.A. Darwish, M. Rashad, A.E. Bekheet, M.M. El-Nahass, J. Alloy. Compd. 709 (2016) 640.
[47] H.E. Atyia, A.E. Bekheet, Phys. B 517 (2017) 19.
[48] I.T. Zedan, M.M. El-Nahass, Appl. Phys. A 120 (2015) 983.
[49] M.S. El-Bana, S.S. Fouad, J. of Applied Physics A 124 (2018) 132.
[50] H.Y. Zahran, I.S. Yahia, F.H. Alamri, Phys. B 513 (2017) 95.
[51] M.M. Abdel-Aziz, I.S. Yahia, L.A. Wahab, M. Fadel, M.A. Afifi, Appl. Surface Science 252 (2006) 8163.
[52] E.G. El-Metwally, M.O. Abou-Helal, I.S. Yahia, J. Ovonic Res. 4 (2008) 20.
[53] S.S. Fouad, I.M. El Radaf, Pankaj Sharma, M.S. El-Bana, J. Alloys Compd 757 (2018) 124.
[54] D.M. Abdel-Basset, S. Mulmi, M.S. El-Bana, S.S. Fouad, Inorg. Chem. 56 (2017) 8865.
[55] M. Losurdo, M.M. Giangregorio, M. Luchena, P. Capezzuto, G. Bruno, R. Gtoro, G. Malandrio, L.I. Fragala, R. Nigro, Appl. Surf. Sci. 253 (2006) 322.
[56] W.M. Desoky, Mahmoud S. Dawood, M.M. El-Nahass, Optik 17 (2019) 351.
[57] A.A. Al-Muntaser, M.M. El-Nahass, A.H. Oraby, M.S. Meikhail, Spectrochim. Acta Part A Mol. Biomol. Spectrosc. 220 (2019) 117112.
[58] F. Yakuphanoglu, M. Sekerci, O.F. Ozturk, Opt. Commun. 239 (2004) 275.
[59] S. Kimura, M. Okuno, H. Iwata, T. Nishi, H. Aoki, A. Ochiai, Phys. B 312–313 (2002) 356.
[60] A.A. Abuelwafa, A. El-Denglawey, M. Dongol, M.M. El-Nahass, T. Soga, J. Alloys Compd 655 (2016) 415.